# Soliton-radiation beat analysis

M. Böhm* and F. Mitschke
*Universität Rostock, Institut für Physik, Rostock, Germany*
(Received 17 March 2006; published 15 June 2006)

A technique is introduced which allows us to extract information on the solitonic content from a nonlinear wave. Its applicability is not as narrowly restricted as that of inverse scattering theory; therefore, it works in situations that could not be studied before. As an example we identify and demonstrate a higher order dispersion-managed soliton.

DOI: 10.1103/PhysRevE.73.066615 PACS number(s): 42.81.Dp, 42.65.Tg

## INTRODUCTION

Solitons and solitary waves are the result of a stable balance between dispersive (or diffractive) and nonlinear effects. The fascination of solitons stems from their property to be "unavoidable:" In any system that can support solitons at all, an initial condition that does not possess quite the right shape of a soliton will excite one nevertheless; even when during propagation the soliton is perturbed, it will heal out once the perturbation ends. This self-adjusting property works not only in simplified mathematical models but equally well in many real-world situations [1]—hence the considerable appeal for applications. Some of the initial energy may not go into the soliton but may be radiated off. In most cases, therefore, a nonlinear wave will contain a solitonic part and radiative background.

We here address the special case of solitons in optical fiber which take the form of picosecond light pulses traveling down the fiber [2,4]. Fiber-optic solitons now find entry into commercial optical telecommunication systems. In this context the radiative part is usually considered as something of a nuisance and has not been studied in much detail (but see [5]). The established method to tell radiative background and one or possibly several solitons apart is the inverse scattering theory (IST) [6]. Since its inception IST has led to many groundbreaking insights into nonlinear waves. IST is an analytical theory, but direct scattering transform, an important step in IST to find the soliton content, can be performed numerically for arbitrary initial conditions [7]. Note, however, that IST is valid only in integrable systems.

Here we introduce a quite different technique serving the same purpose. It is based entirely on numerical procedures. This has the obvious drawback that a single run can only analyze the situation at a particular parameter set, while an analytical result has the undeniable advantage that it immediately provides information on the scaling of results with variation of parameters. This consideration is outweighed, however, by the fact that our method demonstrably works well in many situations in which IST utterly fails: It is applicable much more generally, and in many interesting cases it is the only viable method. Indeed, any situation for which propagation can be modeled numerically seems to be accessible to our method.

The crucial insight at the core of our technique is this: The evolution of a nonlinear wave, unless it happens to be a pure soliton, looks very complicated due to interference between the solitonic content and the radiative background. The interference pattern by necessity contains information on both constituents, but so far it has never been described how this wealth of information can be decoded and utilized. This is exactly what our method accomplishes.

To introduce our method, we first describe its application to a very simple case which can also be treated analytically. This allows us to compare the results of our method with known analytical results. Finally we will proceed to apply the method to a situation which so far has not been accessible at all: In dispersion-managed fibers the dispersion is made to alternate between positive and negative; such fibers are now commercially deployed as a matter of routine. IST is not applicable to dispersion-managed fibers, but we apply our method successfully and thus demonstrate its power. Specifically, we are going to identify a dispersion-managed $(N=2)$-soliton, the existence of which so far has been more or less a matter of conjecture.

## THE FUNDAMENTAL SCHRÖDINGER SOLITON: ANALYTICALLY KNOWN RESULTS

To start with a simple case which can also be solved analytically, we choose here the well known nonlinear Schrödinger equation (NLSE) without any additional higher order terms, which describes the change of the pulse field envelope $A(T,z)$ during propagation in a fiber:

$$\frac{\partial A}{\partial z} = -\frac{i}{2}\beta_2 \frac{\partial^2 A}{\partial T^2} + i\gamma |A|^2 A. \tag{1}$$

Here, $z$ is the distance along the fiber, and $T$ time in the comoving frame. The group velocity dispersion parameter $\beta_2$ and the nonlinearity coefficient $\gamma$ are constant fiber parameters [2]. This equation has, among others, the well-known solution of the fundamental soliton for $\beta_2 < 0$,

$$A(T,z) = \sqrt{\hat{P}}\,\mathrm{sech}\left(\frac{T}{T_0}\right)\exp\left(\frac{i}{2}\gamma \hat{P} z\right) \tag{2}$$

where $A$ is related to the peak power $\hat{P}=|A(0,0)|^2$. Since for a soliton a dynamic equilibrium between dispersive and nonlinear effects is needed, a constraint links $T_0$ and $\hat{P}$; it can be

*Electronic address: michael.boehm@uni-rostock.de

 

written as the "condition of constant action:"

$$T_0^2\hat{P} = \frac{|\beta_2|}{\gamma} = \text{const.} \tag{3}$$

whereas the energy is

$$E = 2T_0\hat{P}. \tag{4}$$

To better deal with multiple solitons and various launch conditions, we now introduce a specific terminology: For all quantities $A$, $E$, $T$ and $\hat{P}$ we introduce double indices, e.g., $T_{jN}$, etc. The first index denotes the $j$th soliton ($j=1,2,3,\ldots$) because below we will consider the simultaneous occurrence of several solitons. $N$ has been called the "soliton order" [8]; it is a positive real number and serves to scale the initial condition with respect to the fundamental soliton. Thus, in the following $T_0 \rightarrow T_{11}$, $A$ and $\hat{P}$ from Eq. (2) become $A_{11}$ and $\hat{P}_{11}$, respectively, and $E$ in Eq. (4) becomes $E_{11}$.

Now we choose a simple initial condition, a sech-shaped unchirped pulse to be launched into the fiber:

$$A_{1N}(T,0) = N\sqrt{\hat{P}_{11}}\,\text{sech}\left(\frac{T}{T_{11}}\right). \tag{5}$$

It has the total energy

$$E_{\text{tot}} = 2N^2T_{11}\hat{P}_{11}. \tag{6}$$

Launching this pulse will result in the formation of solitons, each of which must obey Eq. (3):

$$T_{jN}^2\hat{P}_{jN} = \frac{|\beta_2|}{\gamma} = \text{const.} \tag{7}$$

According to IST the first soliton will be generated above the threshold value of $N=\frac{1}{2}$ [8] and will have the energy

$$E_{1N} = 2T_{1N}\hat{P}_{1N} = (2N-1)E_{11}. \tag{8}$$

Therefore, the duration and peak power, which have to fulfill the conditions (7) and (8), are given by

$$T_{1N} = \frac{1}{2N-1}T_{11} \quad \text{and} \quad \hat{P}_{1N} = (2N-1)^2\hat{P}_{11}. \tag{9}$$

The propagation of the first soliton can, therefore, be described by

$$A_{1N}(T,z) = (2N-1)\sqrt{\hat{P}_{11}}\,\text{sech}\left((2N-1)\frac{T}{T_{11}}\right) \times \exp\left(i\frac{1}{2}\gamma(2N-1)^2\hat{P}_{11}z\right). \tag{10}$$

## PHASE DYNAMICS AND BEAT NOTES

Since we are interested in interference phenomena, the phase dynamics is most important here. We note from Eq. (10) that the phase of a soliton evolves at a time-independent rate proportional to the peak power.

In contrast, the phase evolution of linear (low power nonsolitonic) waves is quite different. Such low-power waves are created from the energy that is shed by solitons in the course of shape readjustment. Their phase is time dependent: They have a parabolic dispersion relation. Therefore, they disperse away from the soliton in the course of time. In the soliton community these waves are, therefore, called radiation.

Typically, solitonic plus radiative waves will exist in a fiber simultaneously. They will therefore beat with each other. The beat pattern is determined chiefly by the phase evolution of both parts. In a more general case, there can be a vast variety of soliton-soliton and soliton-radiation interference terms. Therefore, we will use bracketed upper indices for quantities resulting from interference, like a phase difference $\Delta\phi^{(ab)}$, where $a$ and $b$ are either zero when denoting radiation, or the $j$ value of the involved soliton.

Let us first focus on the interference pattern between the first soliton and the radiation. The interference pattern should repeat after a distance $L^{(10)}$ if the phase difference of the two components

$$\begin{aligned}\Delta\phi^{(10)} &= \Delta\phi_{1N} - \Delta\phi_{\text{rad}} \\ &= [\phi(z+L^{(10)}) - \phi(z)] \\ &\quad - [\phi_{\text{rad}}(z+L^{(10)}) - \phi_{\text{rad}}(z)]\end{aligned} \tag{11}$$

equals $2\pi$. Fortunately only the strictly comoving part of the radiative wave is relevant for the long term interference; its phase is independent of $z$, and can be set to zero without loss of generality. Then, using Eqs. (2) and (10),

$$\begin{aligned}\Delta\phi^{(10)} &= \phi(z+L^{(10)}) - \phi(z) = \frac{\gamma}{2}\hat{P}_{1N}(z+L^{(10)}) - \frac{\gamma}{2}\hat{P}_{1N}z \\ &= \frac{\gamma}{2}\hat{P}_{1N}L^{(10)} = \frac{\gamma}{2}(2N-1)^2\hat{P}_{11}L^{(10)} \stackrel{!}{=} 2\pi.\end{aligned} \tag{12}$$

Now we consider the spatial frequencies of the beat notes, which are of the type

$$Z = \frac{1}{L}; \tag{13}$$

we prefer to denote them by capital $Z$ rather than the more conventional $k$ because we define them as inverse lengths without a factor of $2\pi$.

Specifically, from Eq. (12) we see that here

$$Z^{(10)} = \frac{1}{L^{(10)}} = (2N-1)^2\frac{\gamma\hat{P}_{11}}{4\pi} = (2N-1)^2Z_{\text{sol}}. \tag{14}$$

Here we introduce the spatial frequency of the fundamental soliton $Z_{\text{sol}}$:

$$Z_{\text{sol}} = \frac{\gamma\hat{P}_{11}}{4\pi} = \frac{1}{8z_0}. \tag{15}$$

It is equal to the inverse spatial period of the soliton; the customary definition of the soliton period $z_0$ [2] refers to one eighth of that distance.

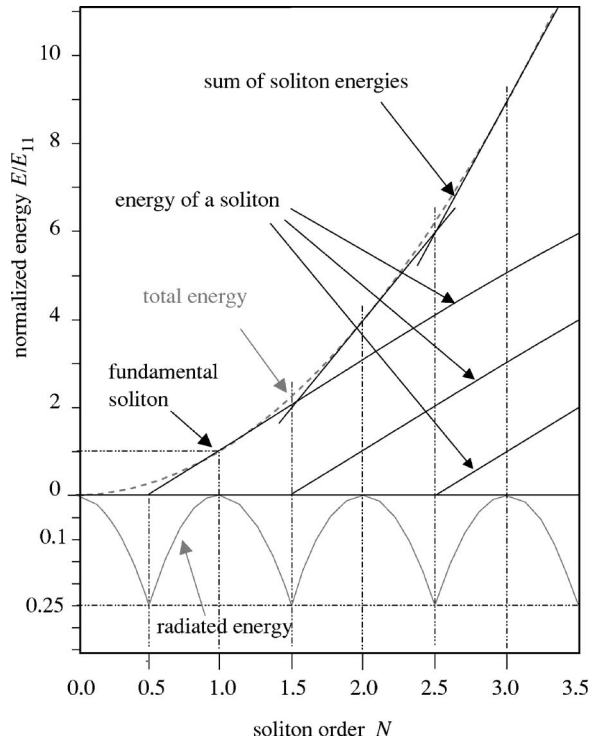


FIG. 1. Soliton content of the input pulse $A(T,0)$ [Eq. (5)]. Upper part: The energy content of each soliton rises linearly beyond its threshold at half-integer $N$ (three parallel slanted lines). The sum is piecewise-linear and approximates the parabola $E_{\mathrm{tot}} \propto N^2$ (dashed). Lower part: The difference between piecewise-linear function and parabola is the radiative energy, shown on an expanded scale. It vanishes at integer $N$ values and has maxima at half-integer points.

Expressing $N$ through pulse energy, Eq. (14) yields a spatial frequency of the beat between the radiation and the first soliton

$$Z^{(10)} = \frac{\gamma \hat{P}_{11}}{4\pi}\left(2\sqrt{\frac{E_{\mathrm{tot}}}{E_{11}}} - 1\right)^2 \tag{16}$$

or alternatively,

$$Z^{(10)} = \frac{T_{11}^2}{4\pi|\beta_2|}\left(2\sqrt{\frac{\gamma T_{11} E_{\mathrm{tot}}}{2|\beta_2|}} - 1\right)^2. \tag{17}$$

These expressions describe the beat spatial frequency in terms of fiber parameters $(\gamma, \beta_2)$ and initial pulse parameters ($E_{\mathrm{tot}}$ and either $T_{11}$ or $\hat{P}_{11}$). Keep in mind that this is valid only for $N > \frac{1}{2}$ or equivalently $E_{\mathrm{tot}} > \frac{2|\beta_2|}{\gamma T_{11}}$.

## EXTENSION TO MULTIPLE SOLITONS

When the input energy is increased beyond what is required for the first soliton, the fractional energy which goes into the radiative background will grow. If it reaches a sufficient amount, it can form another soliton.

We illustrate the situation with Fig. 1. Consider $N$ as the variable to be increased from zero. As soon as $N = \frac{1}{2}$ is reached, a first soliton is generated; its energy increases linearly with $N$ from then on. Once $N = \frac{3}{2}$ is reached, another soliton is created; again, its energy increases linearly. The same repeats at every half-integer $N$. The solitonic energies thus scale as $E_{1N} \propto (2N-1)$, $E_{2N} \propto (2N-3)$, etc.

The sum of the solitonic energies is given by a piecewise-linear function which is tangent to the parabola $E_{\mathrm{tot}} \propto N^2$ [see Eq. (6)] whenever $N$ is integer. The difference between the piecewise-linear solitonic energy and the parabola (total energy) is the radiative energy, and is shown on an expanded scale in the lower part of the figure. For integer $N$ (at the tangent points) the radiative energy vanishes, and all of the initial energy is invested in solitons.

The figure graphically illustrates the solitonic and radiative content for any $N$. For example, at $N=2$ there are two fundamental solitons with energies $E_{11}$ and $3E_{11}$.

In correspondence with Eq. (10) we can now write expressions for the isolated second soliton

$$A_{2N}(T,z) = (2N-3)\sqrt{\hat{P}_{11}}\,\mathrm{sech}\left((2N-3)\frac{T}{T_{11}}\right) \times \exp\left(i\frac{1}{2}\gamma(2N-3)^2\hat{P}_{11}z\right), \tag{18}$$

the third soliton

$$A_{3N}(T,z) = (2N-5)\sqrt{\hat{P}_{11}}\,\mathrm{sech}\left((2N-5)\frac{T}{T_{11}}\right) \times \exp\left(i\frac{1}{2}\gamma(2N-5)^2\hat{P}_{11}z\right), \tag{19}$$

etc. Again, in correspondence with Eq. (16) the beat notes with the radiative background have spatial beat frequencies

$$Z^{(20)} = Z_{\mathrm{sol}}\left(2\sqrt{\frac{E_{\mathrm{tot}}}{E_{11}}} - 3\right)^2 \tag{20}$$

$$Z^{(30)} = Z_{\mathrm{sol}}\left(2\sqrt{\frac{E_{\mathrm{tot}}}{E_{11}}} - 5\right)^2, \tag{21}$$

etc. Since the interference of soliton and radiation is a nonlinear superposition, the interference pattern is not strictly sinusoidal. Therefore, higher harmonics of the different $Z^{(j0)}$ occur at frequencies $lZ^{(j0)}$ with $l$ integer. The first three frequencies and their harmonics up to fifth order are plotted in Fig. 2.

So far we have discussed beat notes between solitons and radiative background. However, as soon as there is more than one soliton, we also need to consider beat notes between the solitons. The spatial beat frequency between the first and second soliton can be calculated from Eqs. (16) and (20) as follows:

$$\begin{aligned} Z^{(12)} &= Z^{(10)} - Z^{(20)} \\ &= Z_{\mathrm{sol}}\left(2\sqrt{\frac{E_{\mathrm{tot}}}{E_{11}}} - 1\right)^2 - Z_{\mathrm{sol}}\left(2\sqrt{\frac{E_{\mathrm{tot}}}{E_{11}}} - 3\right)^2 \\ &= Z_{\mathrm{sol}} 8\left(\sqrt{\frac{E_{\mathrm{tot}}}{E_{11}}} - 1\right) = 8Z_{\mathrm{sol}}(N-1) \end{aligned} \tag{22}$$

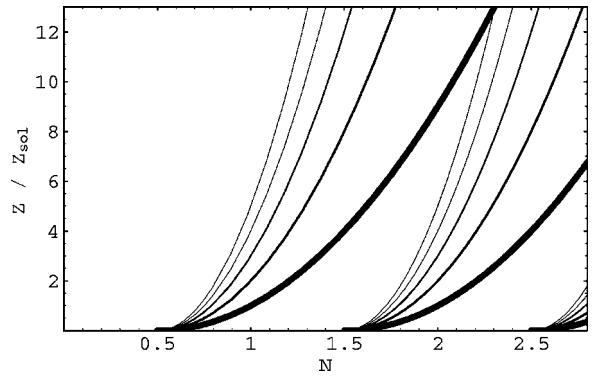


FIG. 2. Dependence of the spatial frequencies $Z^{(j0)}$ of the initial parameter $N$. At every half-integer $N$ a set of traces for the corresponding soliton begins, describing the spatial frequency for the corresponding spectral peak, and its harmonics up to fifth order.

The spatial frequency $Z^{(12)}$ exists for $N>\frac{3}{2}$. At $N=2$ we recover the well-known soliton frequency $Z^{(12)}=8Z_{\mathrm{sol}}=1/z_0$ [compare Eq. (15)].

Figure 3 is an extension of Fig. 2, in that a selection of beat frequencies between solitons has been included. In particular, note the straight line that branches off from the fundamental trace of the first soliton at $N=1.5$, $Z/Z_{\mathrm{sol}}=4$. It represents the difference between the fundamental of the first soliton and the fundamental of the second soliton, $Z^{(12)}=Z^{(10)}-Z^{(20)}$. Also note the curves that bend down: They represent $Z^{(10)}-2Z^{(20)}$, $Z^{(10)}-3Z^{(20)}$, etc.

So far we have rephrased well-known facts in a particular terminology. In the following paragraph we will benefit from this terminology when we introduce our method.

## NUMERICAL BEAT ANALYSIS: THE PROCEDURE

Propagation of an arbitrary light pulse in optical fiber can be numerically computed using established methods. In general one obtains a complicated interference pattern between solitons and radiation. Figure 4 shows an example of a computed propagation, performed using the split-step Fourier method [9]. This pattern is the result of beating between soliton content and radiative waves and must therefore contain information on both. Can useful information on the soliton content be extracted? The answer is in the affirmative.

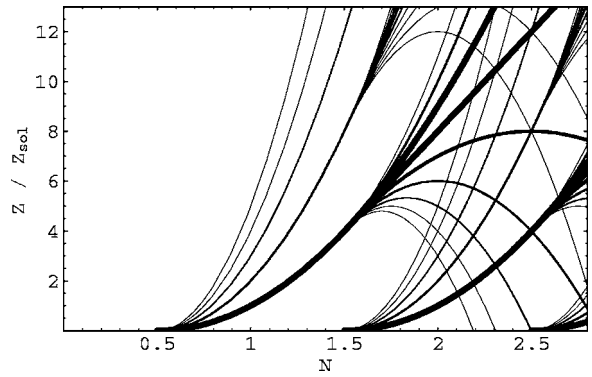


FIG. 3. Further traces have been added to the analytical beat note chart of Fig. 2. Here, combination tones between first, second, and third soliton are shown; in particular, the beat note between the fundamental frequencies of the first and second soliton is highlighted by a bold line. Traces bending down represent difference frequencies between one soliton and overtones of the next.

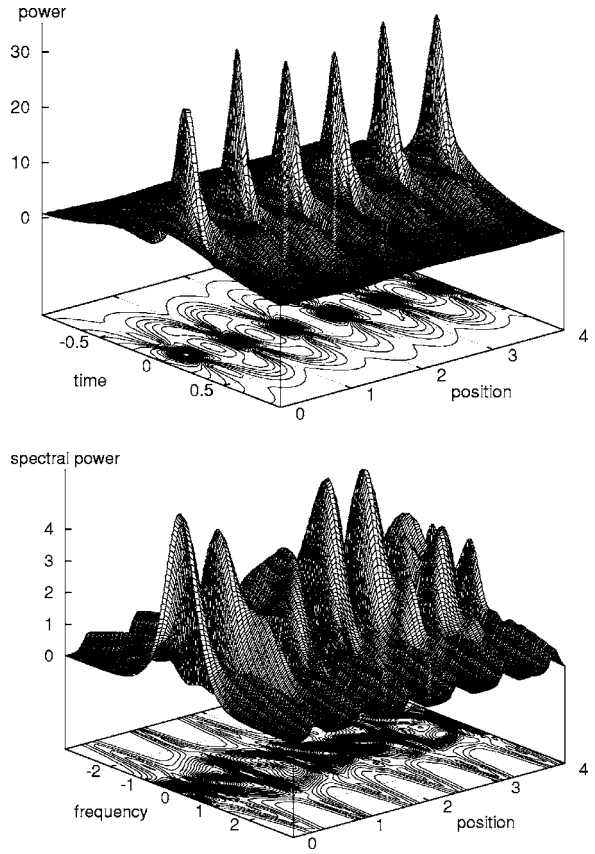


FIG. 4. Example of a complicated beat pattern in both temporal (top) and spectral (bottom) domain. Here the initial condition $A(T,0)$ of Eq. (5) with $N=2.43$ was used.

Treatment of the problem can be simplified if we drastically reduce the amount of data in the beat pattern to a scalar evolution series of single quantity. For this quantity several choices are possible: Peak power, pulse duration, spectral peak power, or spectral width immediately come to mind. While any of these is viable, the spectral peak power will provide the best results. The reason is that as the radiation disperses away from the soliton in the time domain, the overlap between soliton and radiation is reduced. Therefore, the amplitude of the temporal beat note is soon diminished (see Fig. 5). On the other hand, in the spectral domain the soliton as well as the radiation regarded independently will not change their power spectrum, which leads to a persistent beat pattern. Therefore, we pick the spectral power at center frequency $|\tilde{A}(0,z)|^2$ as the scalar quantity.

The next step is to take the Fourier transform of this quantity to identify the spatial frequency content in the beat pattern. It is sufficient to use only the power spectrum, and therefore we ignore the phase spectrum. Figure 6 shows the resulting power spectrum. It contains a multitude of frequencies, which become visible only when the Fourier transform yields sufficient dynamic range. For this reason we find it

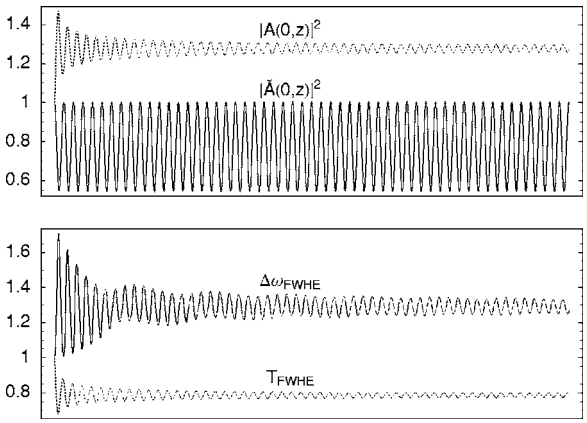


FIG. 5. Comparison of the evolution of peak power $|A(0,z)|^2$, spectral peak power $|\tilde{A}(0,z)|^2$, full width at half energy $T_{\mathrm{FWHE}}(z)$, and spectral full width at half energy $\Delta\omega(z)$. The graph shows the propagation for $N=1.15$ over 256 soliton periods. All traces are normalized to their initial values.

absolutely mandatory here to use a suitable windowing function for data apodization. The perfect windowing function would ensure narrow spectral peaks and good suppression of spurious responses at the same time; in reality there is always a trade-off [10]. We were successful with either a Blackman-Harris windowing function

$$f(m) = 0.358\,75 - 0.488\,29\cos\left(\frac{2\pi m}{M}\right) + 0.141\,28\cos\left(\frac{4\pi m}{M}\right) - 0.011\,68\cos\left(\frac{6\pi m}{M}\right) \tag{23}$$

or a Gaussian

$$f(m) = \exp\left[-\left(\frac{m-\frac{M}{2}}{cM}\right)^2\right]. \tag{24}$$

In either case, there are $M$ data points, and $1 \leqslant m \leqslant M$. The Gaussian has the advantage that the windowing strength can be easily modified by variation of the parameter $c$ according

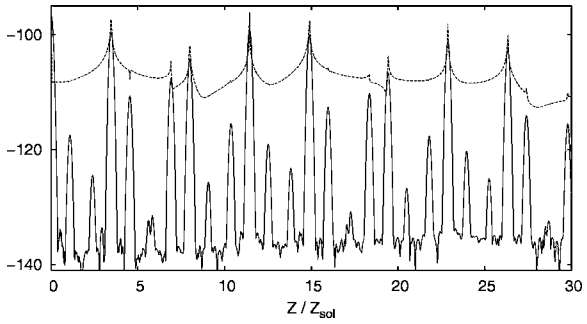


FIG. 6. Fourier transform of the spectral peak power $|\tilde{A}(0,z)|^2$ obtained from $z=0$ to $z=256z_0$ at $N=2.43$. Dashed line: Transform without apodization (rectangular window), solid line: With apodization by a Gaussian with $c=0.12$.

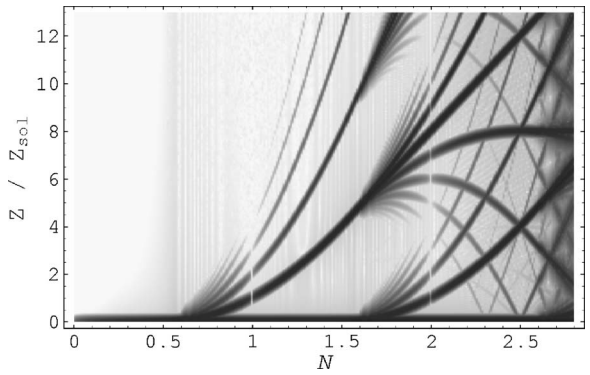


FIG. 7. Numerically evaluated beat note chart for standard fiber. Horizontal coordinate is soliton order, vertical scale is normalized spatial frequency. Each vertical line represents one power spectrum of numerical data. This figure can be directly compared to Fig. 3. Note the narrow vertical white stripes at integer $N$.

to the situation at hand. Typically, $0.05 \leqslant c \leqslant 0.25$, and $c=0.12$ is something of a best compromise where the Gaussian acts with similar strength as the Blackmann-Harris function.

Certainly, the spectrum in Fig. 6 is complicated and seems difficult to decode. The trick is to extend the picture by an additional dimension. Consider how a complicated molecular spectrum is studied by scanning a magnetic field; this causes Zeeman states to move in characteristic ways so that they can be identified. Here we scan the initial pulse parameter $N$. The retrieved spectra are stacked together in Fig. 7, where the spectral power is represented as gray scale. All spectral peaks evolve in characteristic ways with $N$; the way they depend on $N$ indicates their nature, and we can identify them. The reader will notice the close similarity to Fig. 3, which was based on analytical arguments: There is only a continuum below $N=0.5$. At every half-integer $N$ a set of curves begins. Each set consists of a fundamental spatial frequency trace and its overtone traces (compare Fig. 2). With increasing $N$ most spatial frequencies grow.

In contrast to Fig. 3 the traces are interrupted at integer $N$. This can be explained easily: The amplitude of a beat note is proportional to the product of the amplitudes of the two participating waves. In the case of a pure radiationless soliton the radiative wave vanishes (see Fig. 1), and a null in the corresponding beat amplitude results. Those traces that are punctuated by nulls can, therefore, be identified as soliton-radiation beats, the others as soliton-soliton beats. Incidentally, among all beat notes those between the solitons have the highest amplitude.

As a check on the quantitative consistency between the analytical results in Fig. 3 and the numerical data in Fig. 7 we rescale the latter so that one would expect the trace for the fundamental soliton to become a straight line through the origin. Therefore, in Fig. 8 the horizontal axis is rescaled from $N$ to $(2N-1)^2$ [see Eq. (14)]. The result confirms the consistency (correct threshold and scaling exponent) and facilitates identification of the "overtone" of the fundamental soliton trace.

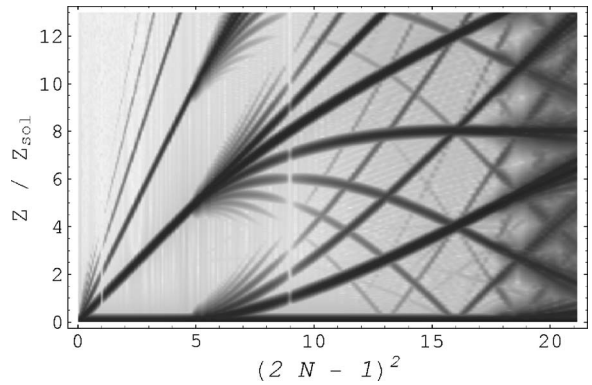


FIG. 8. Beat note chart as in Fig. 7, but rescaled to make the first soliton trace and its overtones straight. The bright stripes now appear at $(2N-1)^2=1$ and 9, respectively.

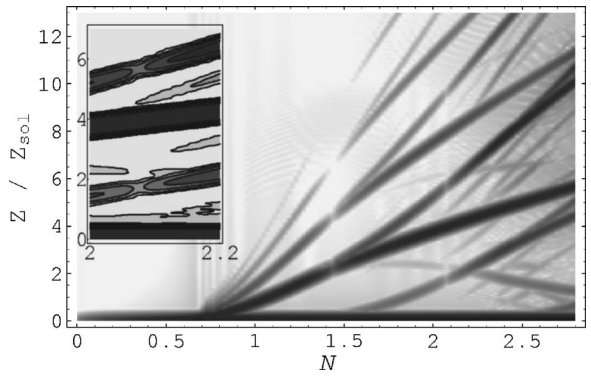


FIG. 9. Fourier-transform of the numerical data: The power spectrum is plotted as a function of the normalized spatial frequency and the soliton order $N$ for a dispersion managed fiber with $S\approx 1.42$. Inset: Enlarged view of traces near $N=2$, rendered as shaded contour plot. This makes it easier to read the coordinates of the minima in two of the traces near $N=2.075$.

## APPLICATION TO MORE REALISTIC CASES

It is straightforward to apply the technique to more complex cases in which corrective terms have been added to the nonlinear Schrödinger equation like, e.g., higher-order dispersion, loss, or Raman terms. Indeed, the procedure remains exactly the same, since it makes no assumptions about integrability. When losses become appreciable over the finite time interval used for the Fourier transform, the transform will return broadened spectral lines. For exceedingly strong losses the Fourier transform does no longer yield meaningful spectral features. However, that is not a flaw of our method, but the result of an ill-posed question.

To demonstrate the power of our method, we now proceed to apply it to a case which can not be treated with conventional methods. A case of considerable current interest is pulse propagation in a dispersion-managed fiber.

To make a dispersion-managed fiber one typically concatenates fibers with different dispersion values so that the dispersion parameter $\beta_2$ periodically alternates between a positive and a negative value. Therefore, the nonlinear Schrödinger equation [Eq. (1)] must be modified by replacing $\beta_2 \rightarrow \beta_2(z)$. Such a fiber is characterized by the path-average dispersion $\beta_{\text{ave}}$, the period length $L_{\text{map}}=L^+ + L^-$, and the map strength [3]

$$S = \frac{|\beta_2^+ - \beta_{\text{ave}}|L^+ + |\beta_2^- - \beta_{\text{ave}}|L^-}{\tau^2} \tag{25}$$

where $\tau$ is the pulse duration (full width at half maximum). $S=0$ recovers the homogenous case.

After the original idea of dispersion management [11] attempts have been made to mathematically describe the propagation [12] or the shape [13,14] of the soliton. IST fails in this situation: $\beta_2$ is a function of $z$ but cannot be replaced—not even approximately—by $\beta_{\text{ave}}$. Whether a viable adaptation of IST will ultimately be found or not, our method avoids such difficulties because it relies on numerical propagation which is straightforward.

In real systems it may be difficult to create the required pulse shape and chirp at the chosen launch point to generate an ideal dispersion managed soliton. As an initial condition we here choose a chirp free Gaussian-shaped pulse which is closer to the DM soliton than a sech-shaped pulse [14]:

$$A(T,0) = NA(0,0)\exp\left(-\frac{1}{2}\left(\frac{T}{T_{11}}\right)^2\right). \tag{26}$$

$A(0,0)$ is the square root of the peak power of a soliton with $S=0$. We launch this pulse at a chirp-free point of the dispersion map [15] and use $S=1.424$ and $N\approx 1.40$. Most of the power is incorporated into the soliton; only $10^{-5}$ of the total launched energy ends up as radiation. Therefore, Eq. (26) provides a remarkably good approximation to the DM soliton shape. The spatial beat note diagram for this case is shown in Fig. 9.

The first observation is about the onset of the first soliton. It is difficult to read precise threshold values because the traces have a certain width and, at the branching point, are tangent to each other. In any event, the first soliton branch in Fig. 9 is shifted to higher $N$ values in comparison to Fig. 7. Also, the characteristic nulls in the traces, indicative of a pure soliton, occur not at $N=1$ but at $N\approx 1.45$. This behavior is well known and is referred to as power enhancement [16–18].

Figure 9 also shows clearly that at $N\approx 1.5$ a second soliton sets in. Similar as above, the spectral peak $Z^{(12)}$ then becomes the most prominent one. A remarkable observation concerns $N\approx 2.075$: The amplitude of each soliton-radiation beat note $Z^{(j0)}$ goes through a deep minimum, while the soliton-soliton beats do not. This is a clear signature of a nearly pure second-order soliton. It has been uncertain to date whether a second order dispersion managed soliton ("$N=2$ DM soliton") exists, but our method can easily reveal its existence and determine its parameters. From Fig. 9 we obtain $Z/Z_{\text{sol}}=5.68$ and 1.73, respectively, at $N=2.075$. Making use of the fact that the nonlinear phase evolution as described by the phase term in Eq. (2) is not affected by dispersive effects, this translates into a ratio of peak powers of the two individual solitons of 3.3 : 1 (compare the homogenous case with 9 : 1). With this information we plot the pure $N=2$ DM soliton in Fig. 10.

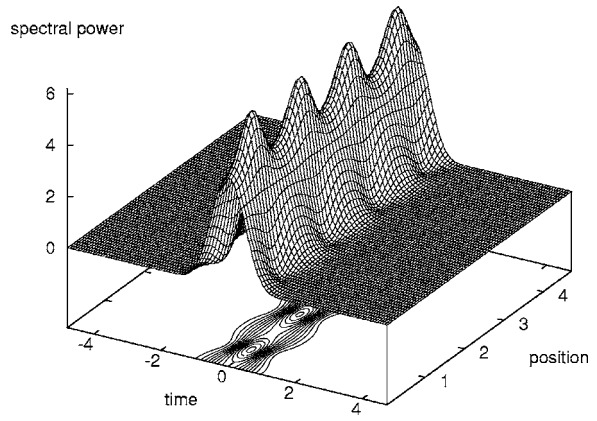


FIG. 10. A pure second-order dispersion managed soliton discovered with the new method. Parameters can be read from inset of Fig. 9; see text.

## DISCUSSION

We introduce a technique that permits the evaluation of the soliton content in a complex nonlinear wave. Since the starting point of the method is a numerical simulation it is nearly universally applicable.

However, it requires a certain finite sample length as a basis for the Fourier transform. A long sample affords better spectral resolution, which may be desirable for elevated $N$ values where a multitude of beat notes becomes increasingly difficult to identify. The use of extended samples is uncritical for a stationary case. In contrast, in the presence of gradual changes of soliton content, e.g., due to energy loss, choice of sample length involves a trade-off between conflicting requirements: A long sample suffers more from the gradual change, and one must balance uncertainties in position and spatial frequency.

IST makes stationarity a precondition, and thus there is no such spatial uncertainty. As a result, IST immediately provides soliton parameters for all $z$ up to $\infty$. Our method is not subject to such preconditions. The price to pay is that (1) information obtained is only valid for the finite spatial interval under consideration (but this is a consequence of the nonstationarity of the problem, not of the technique), and (2) the user must make a meaningful choice of the sample length. It is a matter of future considerations whether in critical cases wavelet transforms may provide improvements.

IST also provides velocity of the solitons. We found an extension of the method presented here that allows the same information to be extracted; however, a discussion must be the subject of a forthcoming publication.

Our technique is most valuable in situations where there are no other techniques available. As an example, we have identified a dispersion-managed higher-order soliton; even the existence of this soliton was uncertain before. It is probable that our technique can also be extended to other nonlinear wave equations, like Korteweg-de Vries, etc.

## ACKNOWLEDGMENTS

This work was supported in the framework of DIP 6.6 (Deutsch-Israelische Projektpartnerschaft).

[1] C. R. Menyuk, Phys. Rev. A **33**, 4367 (1986).
[2] G. P. Agrawal, *Nonlinear Fiber Optics* (Academic, San Diego, 1995).
[3] A. Hasegawa and M. Matsumoto, *Optical Solitons in Fibers* (Springer, Berlin, 2003).
[4] L. F. Mollenauer and J. P. Gordon, *Solitons in Optical Fibers: Fundamentals and Applications* (Elsevier Academic Press, Burlington, MA, 2006).
[5] J. P. Gordon, J. Opt. Soc. Am. A **9**, 91 (1992).
[6] V. E. Zakharov and A. B. Shabat, Sov. Phys. JETP **34**, 62 (1971).
[7] G. Boffeta and A. R. Osborne, J. Comput. Phys. **102**, 252 (1992).
[8] J. Satsuma and N. Yajima, Suppl. Prog. Theor. Phys. **55**, 284 (1974).
[9] R. H. Hardin and F. D. Tappert, SIAM Rev. **15**, 423 (1973).
[10] F. J. Harris, Proc. IEEE **66**, 51 (1978).
[11] M. Suzuki, I. Morita, N. Edagawa, S. Yamamoto, H. Taga, and S. Akiba, Electron. Lett. **31**, 2027 (1995).
[12] I. R. Gabitov and S. K. Turitsyn, Opt. Lett. **21**, 327 (1996).
[13] P. M. Lushnikov, Opt. Lett. **26**, 1535 (2001).
[14] I. Gabitov, E. G. Shapiro, and S. K. Turitsyn, Phys. Rev. E **55**, 3624 (1997).
[15] M. Matsumoto, Opt. Lett. **22**, 1238 (1997).
[16] N. J. Smith, F. M. Knox, N. J. Doran, K. J. Blow, and I. Bennion, Electron. Lett. **32**, 54 (1996).
[17] N. J. Smith, N. J. Doran, F. M. Knox, and W. Forysiak, Opt. Lett. **21**, 1981 (1996).
[18] T.-S. Yang and W. L. Kath, Opt. Lett. **22**, 985 (1997).